**RAA 2014** Vol. **14** No. **6**, 635–647 doi: 10.1088/1674–4527/14/6/003
*http://www.raa-journal.org* *http://www.iop.org/journals/raa*

*Research in Astronomy and Astrophysics*

# Cosmic microwave background constraints on the tensor-to-scalar ratio

King Lau, Jia-Yu Tang and Ming-Chung Chu

Department of Physics and Institute of Theoretical Physics, The Chinese University of Hong Kong, Hong Kong, China; *klau@phy.cuhk.edu.hk*

Received 2013 October 22; accepted 2013 December 27

**Abstract** One of the main goals of modern cosmic microwave background (CMB) missions is to measure the tensor-to-scalar ratio $r$ accurately to constrain inflation models. Due to ignorance about the reionization history $X_e(z)$, this analysis is usually done by assuming an instantaneous reionization $X_e(z)$ which, however, can bias the best-fit value of $r$. Moreover, due to the strong mixing of B-mode and E-mode polarizations in cut-sky measurements, multiplying the sky coverage fraction $f_{\rm sky}$ by the full-sky likelihood would not give satisfactory results. In this work, we forecast constraints on $r$ for the *Planck* mission taking into account the general reionization scenario and cut-sky effects. Our results show that by applying an N-point interpolation analysis to the reionization history, the bias induced by the assumption of instantaneous reionization is removed and the value of $r$ is constrained within $5\%$ error level, if the true value of $r$ is greater than about 0.1.

**Key words:** cosmology: cosmic microwave background — cosmology: cosmological parameters — cosmology: early universe — gravitational waves

## 1 INTRODUCTION

Inflation (Guth 1981; Linde 1982; Albrecht & Steinhardt 1982) is now the leading paradigm in cosmology. The inflation scenarios have been proposed to solve the problems of horizon, flatness and magnetic monopoles and explain the generation of primordial perturbations in the early Universe. Most inflation models predict two types of initial perturbations: scalar and tensor. The scalar perturbations are adiabatic, nearly Gaussian and close to being scale-invariant, which are consistent with a series of observations (Hu & White 1996; Spergel & Zaldarriaga 1997; Hu et al. 1997; Peiris et al. 2003; Spergel et al. 2007; Hinshaw et al. 2013). The tensor perturbations produced during inflation, also known as gravitational waves, can be quantified as a tensor-to-scalar ratio $r$. Therefore, a non-zero $r$ is considered to be important evidence of inflation if it is observed. Since tensor perturbations can be detected in a large-scale temperature power spectrum and should have left an imprint on the B-mode polarization of the cosmic microwave background (CMB) (Seljak & Zaldarriaga 1997; Kamionkowski et al. 1997), constraining $r$ is one of the main goals of modern CMB surveys. Recent data from the nine year result of the Wilkinson Microwave Anisotropy Probe (WMAP9) and South Pole Telescope give the latest constraints of $r < 0.13$ and $r < 0.11$ at the 95% confidence level (CL) respectively without a measurement of the B-mode polarization (Story et al. 2013; Hinshaw et al. 2013; Bennett et al. 2013). Although *Planck*'s results were released in March 2013 (Planck

Collaboration 2013a), its polarization data, which are crucial for constraints on $r$, are not yet available. Their current approach combines *Planck*'s measurements of temperature anisotropy with the WMAP large-angle polarization to constrain inflation, giving an upper limit of $r < 0.11$ as a 95% CL (Planck Collaboration 2013b).

These constraints for $r$ were obtained by assuming an instantaneous model for reionization history, but $X_e(z)$, the average ionized fraction at redshift $z$, is rather uncertain. Various sources such as star formation (Springel & Hernquist 2003; Bunker et al. 2004), massive black holes (Sasaki & Umemura 1996) and dark matter decay (Mapelli et al. 2006; Belikov & Hooper 2009) have been suggested to provide the energy flux necessary for reionizing hydrogen. CMB and quasar observations show that recombination occurs at redshift $z_* \sim 1100$ and the Universe must have been fully reionized at $z \sim 6$ (Becker et al. 2001; Fan et al. 2002), but there is no detailed knowledge about the evolution of $X_e(z)$ between these two eras. The constraint imposed on $X_e(z)$ by current CMB measurements is also poor. The CMB temperature power spectrum $C_l^{\rm TT}$ only gives a strong constraint on $A_{\rm s}e^{-2\tau}$, where $A_{\rm s}$ and $\tau$ are the scalar amplitude and optical depth respectively. Even if we can break the degeneracy between these two parameters, we can only get the information from $\tau$, where

$$\tau \propto \int_0^{z_*} \left(X_e(z)\sqrt{1+z}\right) dz\,, \tag{1}$$

but not $X_e(z)$ itself. The CMB E-mode polarization spectrum $C_l^{\rm EE}$ only has a weak dependence on the reionization history, and thus an attempt at constraining $X_e(z)$ by the current E-mode polarization measurement does not give any satisfactory result (Lewis et al. 2006).

Several studies have considered the effects of uncertainties in $X_e(z)$ on cosmological parameter estimation. To parameterize the reionization history, Lewis et al. assume a constant ionization fraction in finite redshift bins and join the bins using a tanh function (Lewis et al. 2006). Mortonson et al. propose that the reionization history can be expressed as a linear combination of finite numbers of principal components $S_\mu$ extracted from the Fisher information matrix that describes the dependence of E-mode polarization on reionization, so that the amplitudes of $S_\mu$ are parameters for $X_e$ (Mortonson & Hu 2008b). To consider the general reionization scenario, Pandolfi et al. apply these two methods in their analysis to constrain the inflation parameters by WMAP7 data (temperature and E-mode polarization only) (Pandolfi et al. 2010) while the PLANCK Collaboration (Planck Collaboration 2013b) only adopts the method by Mortonson et al. A recent study investigates how instantaneous-like reionization models affect the estimation of all cosmological parameters from *Planck*-quality CMB data except for $r$ (Moradinezhad Dizgah et al. 2013). To account for the fact that parts of the sky are masked to eliminate foreground contaminations, they multiply the sky coverage fraction $f_{\rm sky}$ ($f_{\rm sky} = 0.65$ for *Planck*) by their full-sky likelihood.

In this paper, we explore how well $r$ can be constrained by the *Planck* mission with a general parametrization of the reionization history. In Section 2, we discuss the degeneracy between the reionization history $X_e(z)$ and $r$ in the full-sky CMB power spectra and the necessity of using both temperature and polarization power spectra for constraining $r$. Then we make a full-sky forecast and conclude that a bias is possibly introduced in $r$ if an incorrect reionization assumption is applied in the Markov Chain Monte Carlo (MCMC) analysis (Kosowsky et al. 2002). The N-point linear interpolation method for reionization is also introduced. We then discuss the significance of strong mixing of E-mode and B-mode polarizations and show that the simple $f_{\rm sky}$ modification is unrealistic in constraining $r$ using cut-sky power spectra in Section 3. Thus we apply the Hamimeche and Lewis likelihood approximation which can handle the CMB temperature-polarization correlation for high $l$'s in the cut-sky. In Section 4, we present the forecast of *Planck*'s constraint on $r$ using a general reionization representation.

## 2 DEGENERACY AMONG REIONIZATION HISTORY, $n_{\rm T}$, $r$ AND $n_{\rm s}$

In this study, we consider single-field inflation with the slow-roll approximation. Conventionally, the power spectra of scalar perturbations $P_{\mathcal{R}}$ and tensor fluctuations $P_h$ have the functional form

$$k^3 P_{\mathcal{R}}(k) \propto k^{n_{\rm s}-1}, \tag{2}$$

$$k^3 P_h(k) \propto k^{n_{\rm T}}, \tag{3}$$

in which $n_{\rm s}$ and $n_{\rm T}$ are the spectral index and tensor tilt, respectively. Hence, the tensor-to-scalar ratio $r$ is defined as

$$r \equiv \frac{P_h(k_0)}{P_{\mathcal{R}}(k_0)}, \tag{4}$$

where $k_0$ is the pivot scale. Our choice for it is $k_0 = 0.002$ Mpc$^{-1}$. Moreover, in the simple slow-roll inflation model, there is a well-known consistency relation (Kinney 1998)

$$n_{\rm T} = -\frac{r}{8}, \tag{5}$$

which is correct at first order in the slow-roll parameters. These parameters are of interest for studying the CMB because they give an accurate measurement of $r$ and spectral index $n_{\rm s}$ can discriminate among inflation models (Dodelson et al. 1997; Kinney 1998).

Previous analysis of CMB data usually assumes the reionization history to be instantaneous,

$$X_e(z) \propto \frac{1}{2} + \frac{1}{2}\tanh\left(\frac{z_{\rm re} - z}{\Delta_z}\right), \tag{6}$$

where $\Delta_z$ is a width parameter and $z_{\rm re}$ is the redshift at which reionization occurs. Here, we take $\Delta_z = 1.5$. Combining Equation (6) with Equation (1), we can utilize CMB data to make an inference for the parameters $z_{\rm re}$ and $\tau$. However, it has been pointed out that $C_l^{\rm EE}$ and $C_l^{\rm TE}$, unlike $C_l^{\rm TT}$, depend not only on $\tau$ but also on the detailed evolution of $X_e(z)$ (Lewis et al. 2006), especially for $l < 30$. To compare the impacts of the reionization history on CMB polarization power spectra, we consider the instantaneous model and two other physically acceptable reionization models, double reionization and two-step reionization, as illustrated in Figure 1. The former model has two instantaneous reionizations occurring at $z = 7, 17$ and a sudden, midway recombination, while the latter describes a reionization process with a long, intermediate pause. All of them give $\tau = 0.089$ and are assumed to reach full H ionization at $z \sim 6$, as well as a late time He reionization at $z \sim 3$. The corresponding $C_l^{\rm EE}$, $C_l^{\rm TE}$ and $C_l^{\rm BB}$ are shown in Figure 2. The distinct differences in the three curves for $l < 30$ indicate the dependences of CMB polarization power spectra on the reionization history $X_e(z)$. Although double reionization is rather disfavored by current observations (Zahn et al. 2012), it helps to demonstrate the bias on $r$ if an incorrect reionization model is used.

To examine the possible bias of parameters by an incorrect reionization model, we run a simple test on two sets of full-sky CMB power spectra that have quality comparable to *Planck*. These two sets of power spectra are generated using the standard WMAP9 best-fit cosmological parameters but with the two-step reionization and double reionization model respectively. Meanwhile, we still use an instantaneous reionization model and perform MCMC analysis to estimate $\tau$ from these power spectra (refer to Sect. 4 for details about MCMC fitting).

Figure 3 shows the probability functions of $\tau$ and $z_{\rm re}$ after marginalizing over all other parameters. The dashed and dashed-dotted lines indicate the results using two-step reionization and double reionization, respectively. Both probability functions show a sharp convergence, but a bias in $\tau$ is introduced relative to the fiducial value of the optical depth $\tau = 0.089$, indicated by the vertical line. Moreover, the bias with the double reionization is larger, which reflects the larger difference between the instantaneous model and the double reionization model. As there is a $\tau - n_{\rm T}$ degeneracy

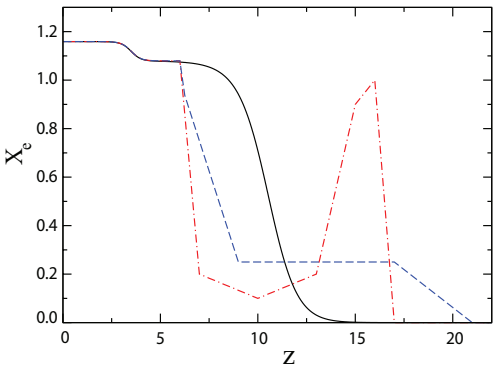


**Fig. 1** The three fiducial reionization models considered in this paper: instantaneous reionization (*solid line*), two-step reionization (*dashed line*) and double reionization (*dash-dotted line*). All of them are assumed to reach full H ionization at $z \sim 6$ and have late time He reionization at $z \sim 3$. All of them give $\tau = 0.089$.

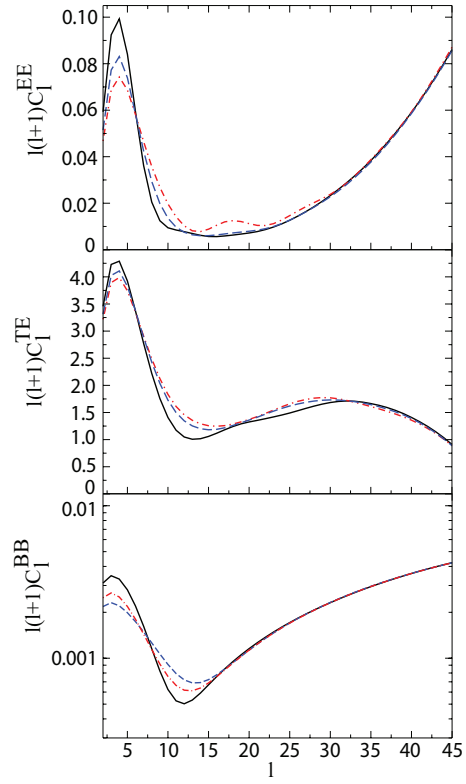


**Fig. 2** The CMB E-mode polarization power spectrum, temperature-E cross spectrum and B-mode polarization power spectrum (all generated by standard ΛCDM best-fit WMAP9 parameters with $r = 0.1$) for three reionization histories: instantaneous (*solid line*), two-step (*dashed line*) and double reionization (*dash-dotted line*) as shown in Fig. 1. They are sensitive to the reionization history for $l \leq 30$.

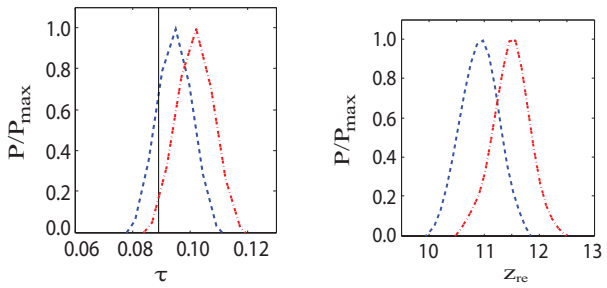


**Fig. 3** Probability functions $P$ (relative to the peak value $P_{\rm max}$) of the MCMC fitting results for the optical depth $\tau$ (*left*) and reionization redshift $z_{\rm re}$ (*right*) from two sets of expected *Planck* full-sky CMB power spectra (including temperature and polarization). We calculate these power spectra using the two-step reionization (*dashed line*) and double reionization (*dash-dotted line*), while assuming the instantaneous reionization history to make the MCMC fitting. Both probability functions show a sharp convergence but a bias is introduced relative to the fiducial value of the optical depth ($\tau = 0.089$) indicated by the vertical line.

on the B-mode polarization spectrum (Mortonson & Hu 2008a), if $\tau$ is biased to a larger value, the corresponding $n_{\rm T}$ becomes less negative; because $r$ and $n_{\rm T}$ are correlated in CMB constraints, a bias in the estimation of $r$ is introduced.

Therefore, to avoid any assumption on reionization history, we modify an N-point parametrization of reionization which was initially proposed by Lewis et al. (2006). We fix $X_e(z = 6) = 1.08$ (with He reionization) and $X_e(z = 22) = 0$, and we insert $N$ floating point values $\{X_e(z_i)\}_{i=1}^{N}$ at redshift

$$z_i = 6 + i(22 - 6)/(N + 1), \qquad i = 1, \cdots, N. \tag{7}$$

Then the whole reionization history in $6 \leq z \leq 22$ is the linear interpolation among these points. This method introduces $N$ reionization points, which are extra parameters in the MCMC analysis together with the cosmological parameters, and they are free to vary in the range [0,1] (the physical range of $X_e(z)$). We assume a late-time He reionization occurred at $z \sim 3$.

## 3 LIKELIHOOD OF CUT-SKY CMB

To make a forecast from fiducial CMB power spectra, we perform a TT-TE-EE-BB joint analysis covering both small and large scales with the N-point method. It is important to include the $C_l^{\rm TT}$ power spectrum to constrain the baryonic density $\Omega_{\rm b}$, dark matter density $\Omega_c$, Hubble parameter $H$ and $A_{\rm s}e^{-2\tau}$ well. As tensor perturbations contribute to the CMB temperature power spectrum at large scales, its effect is degenerate with the change in $n_{\rm s}$ in large-scale CMB measurements. Therefore, the $C_l^{\rm TT}$ power spectrum at small scales can help break this degeneracy by constraining $n_{\rm s}$ well. It is also necessary to include $C_l^{\rm EE}$ and $C_l^{\rm BB}$ power spectra at large scales, and drop the assumption of instantaneous reionization to break the $\tau - r$ degeneracy as we discussed in Section 2. Although $C_l^{\rm TE}$ has a weak dependence on reionization history, as it is a cross spectrum, its noise is much reduced, and thus it helps to break this degeneracy in a joint analysis.

Assuming that the CMB field is Gaussian and isotropic, the full-sky maximum likelihood $\mathcal{L}$ for the measured TEB correlation spectra $\hat{C}_l$ is

$$-2\ln\mathcal{L} = \sum_{l_{\rm min}}^{l_{\rm max}}(2l + 1)[{\rm Tr}(\hat{\mathbf{C}}_l\mathbf{C}_l^{-1}) - \ln|\hat{\mathbf{C}}_l\mathbf{C}_l^{-1}| - 3], \tag{8}$$

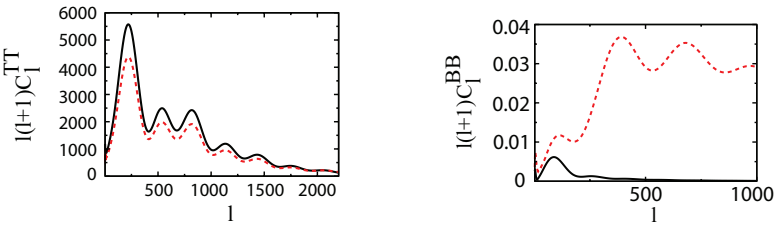


**Fig. 4** The CMB temperature (*left*) and B-mode polarization power spectrum (*right*) for full-sky (*solid lines*) and their pseudo power spectra for cut-sky (*dashed lines*), for the fiducial model of $r = 0.1$ and standard cosmological parameters. $P(C_l^{\rm BB})$ is increased by the mask due to mixing with $C_l^{\rm EE}$, making the simple $f_{\rm sky}$ modification unrealistic. The masks applied by WMAP are used in this illustration.

where

$$\mathbf{C}_l = \begin{pmatrix} C_l^{\rm TT} & C_l^{\rm TE} & C_l^{\rm TB} \\ C_l^{\rm TE} & C_l^{\rm EE} & C_l^{\rm EB} \\ C_l^{\rm TB} & C_l^{\rm EB} & C_l^{\rm BB} \end{pmatrix} \tag{9}$$

is the matrix of theoretical power spectra and $\hat{\mathbf{C}}_l$ is defined similarly.

In practice, masks are applied for both temperature and polarization data (Jarosik et al. 2011), to exclude the part of the sky map contaminated by the astrophysical foreground, mainly the Galactic plane. To have a cut-sky forecast, the sky coverage fraction $f_{\rm sky}$ is usually included as a factor in Equation (8) to account for the fractional loss of $\hat{C}_l$ power spectra in the cut-sky. While $f_{\rm sky}$ modification works well for the temperature power spectrum, it is not sufficient for the polarization spectra, but the $C_l^{\rm BB}$ power spectrum is crucial for the constraint of $r$. Burigana et al. have considered a toy model to include the impact of the foreground contamination in full-sky likelihood analysis (Burigana et al. 2010). This method, however, will introduce uncertainties in modeling the noise residuals and therefore $r$ and $X_e$. With this consideration, in this work, we use the pseudo-$C_l$ as the estimators and apply the likelihood approximation introduced by Hamimeche and Lewis (hereafter H.L. likelihood) (Hamimeche & Lewis 2008). The pseudo power spectrum $P(C_l)$, defined as the power spectrum over a masked sky map, is related to the full-sky CMB spectrum by the relation (Kogut et al. 2003)

$$\left\langle \begin{pmatrix} P(C_l^{\rm TT}) \\ P(C_l^{\rm TE}) \\ P(C_l^{\rm EE}) \\ P(C_l^{\rm BB}) \end{pmatrix} \right\rangle = \sum_{l'} \begin{pmatrix} M_{ll'}^{\rm TT} & 0 & 0 & 0 \\ 0 & M_{ll'}^{\rm TE} & 0 & 0 \\ 0 & 0 & M_{ll'}^{\rm EE} & M_{ll'}^{\rm EB} \\ 0 & 0 & M_{ll'}^{\rm BE} & M_{ll'}^{\rm BB} \end{pmatrix} \begin{pmatrix} C_{l'}^{\rm TT} \\ C_{l'}^{\rm TE} \\ C_{l'}^{\rm EE} \\ C_{l'}^{\rm BB} \end{pmatrix}, \tag{10}$$

where $\langle ... \rangle$ denotes the expectation value and $\{M_{ll'}^{XY}\}$ are the coupling mask matrices. Details about this likelihood are described in the Appendix.

Before we proceed, we illustrate in Figure 4 why a simple $f_{\rm sky}$ modification of the full-sky likelihood would not give a realistic constraint on $r$. Figure 4 compares the full-sky $C_l^{\rm TT}$ and $C_l^{\rm BB}$ (solid lines) and their corresponding pseudo power spectrum in the cut-sky (dashed lines), for $r = 0.1$. We apply the same masks released by the WMAP team[1], which are equivalent to $f_{\rm sky} = 0.65$. As expected, $P(C_l^{\rm TT})$ is approximately reduced by a factor of $f_{\rm sky}$ compared with $C_l^{\rm TT}$. However, $P(C_l^{\rm BB})$ is significantly increased, due to the mixing between $C_l^{\rm EE}$ and $C_l^{\rm BB}$ and the coupling among different $l$-modes.

[1] The masks for WMAP are available at *http://lambda.gsfc.nasa.gov/product/map/dr4/masks_get.cfm*

## 4 FORECAST FOR *PLANCK*

To forecast the constraints on $r$ by the *Planck* survey with a general reionization scenario, we perform MCMC analysis with the H.L. likelihood discussed in the Appendix. The expected *Planck* pseudo power spectra $\hat{C}_l$ from the fiducial power spectra $C_l^{\rm fid}$ are calculated as

$$\hat{C}_l^{XY} = P(b_l^2 C_l^{{\rm fid}XY} + N_l^{XY}) \tag{11}$$

for $X, Y = T, E$ or $B$, where

$$b_l^2 = \exp\left(\frac{-l(l+1)(\theta_{\rm fwhm}/{\rm rad})^2}{8{\rm ln}2}\right), \tag{12}$$

the beam width $\theta_{\rm fwhm} = 7.1'$ and the noises $N_l^{XY}$ for the $C_l^{XY}$ spectrum are $N_l^{\rm TT} = 1.5 \times 10^{-4}\ \mu{\rm K}^2$, $N_l^{\rm EE} = N_l^{\rm BB} = 3.61 N_l^{\rm TT}$ (PLANCK Collaboration 2006) and $N_l^{\rm TE} = 0$. We use the frequency band centered at 143 GHz and assume that there is no correlation among the random noise fields. $C_l^{\rm fid}$ is computed using CAMB[2] (Lewis et al. 2000). The fiducial model used to compute $C_l^{\rm fid}$ is $\Omega_b h^2 = 0.0227, \Omega_c h^2 = 0.108, n_{\rm s} = 0.961, 100\theta = 1.040137$ and $A_{\rm s} = 2.41 \times 10^{-9}$, using standard notations for the cosmological parameters. Two fiducial models of reionization, the double reionization and two-step reionization, are considered in our analysis, which are shown in Figure 1. In addition, we investigate three cases for $r$: $r = 0.05, 0.1$ and $0.15$ and their corresponding tensor tilt is taken as $n_{\rm T} = -r/8$. Thus, six sets of pseudo power spectra $\hat{C}_l^{XY}$ are generated.

We perform the MCMC analysis using the modified version of CosmoMC[3] (Lewis & Bridle 2002) by Mortonson and Hu[4] (Mortonson & Hu 2008a). To study the impact of reionization history on estimation as discussed in Section 2, two treatments on $X_e$ are applied. For the first, we use the instantaneous reionization modeled as in Equation (6). The varied parameters are $\{\Omega_b h^2, \Omega_c h^2, \theta, n_{\rm s}, n_{\rm T}, \log(10^{10} A_{\rm s}), r, \tau\}$. The second treatment uses the N-point method defined in Equation (7); we further modify the CosmoMC program to vary parameters $\{\Omega_b h^2, \Omega_c h^2, \theta, n_{\rm s}, n_{\rm T}, \log(10^{10} A_{\rm s}), r, \{X_e(z_i)\}_{i=1}^N\}$ for $N = 7$. The likelihood is summed over $l_{min} = 2$ and $l_{\rm max} = 2200$. We are aware that the H.L. likelihood is less reliable for pseudo-$C_l$ at low-$l$ range, and Hamimeche & Lewis (2008) state that exact likelihood calculation is feasible at low-$l$ when realistic foreground contamination is carefully considered. However, this investigation is beyond the scope of this paper. In addition, the CMB polarization power spectra at low-$l$ are essential for breaking the degeneracy between the reionization history and inflation parameter $r$. Our results show that if $l_{\rm min}$ is taken as 10, only $\tau$ is biased by $\sim 1\sigma$ by the choice of $l_{\rm min}$ (smaller $l_{\rm min}$ gives a better constraint), while similar best-fit values of $r$ and other cosmological parameters with slightly larger uncertainties are obtained. Therefore, we extend the application of H.L. likelihood to $l_{\rm min} = 2$ and focus on the results based on this condition.

Figure 5 and Figure 6 compare the constraints on $r$ by the N-point method and the instantaneous model. The left and right panels of these plots show the results for the fiducial $r = 0.1$ and $r = 0.15$, respectively. The statistics describing them, including best-fit, mean $\bar{r}$, standard deviation $\sigma$ and CL, are shown in Tables 1 and 2. It can be seen that for a complex reionization history, the simple instantaneous assumption generally biases $r$ to a smaller value. In our case, the true value of $r$ is even ruled out at the 68% CL for both double-step reionization and two-step reionization models. The application of the N-point method can correct for these biases and the best-fit value of $r$ is constrained to within the 5% error level if the true value of $r \gtrsim 0.1$. The N-point method also gives a better inference on $\bar{r}$.

[2] CAMB is available at *http://camb.info/*

[3] CosmoMC is available at *http://cosmologist.info/cosmomc/*

[4] Mortonson and Hu's program is available at *http://background.uchicago.edu/camb_rpc/*

**Table 1** Statistics of 1D marginalized probability of $r$ for MCMC analysis on the expected *Planck* pseudo power spectra with double reionization.

| Fiducial $r$ | Reionization model | Best-fit | $\bar{r} \pm \sigma$ | 68% CL | 95% CL |
|---|---|---|---|---|---|
| 0.1 | Instantaneous | 0.048 | $0.074 \pm 0.043$ | [0, 0.092] | [0, 0.152] |
| 0.1 | N-point | 0.095 | $0.102 \pm 0.045$ | [0, 0.122] | [0, 0.178] |
| 0.15 | Instantaneous | 0.143 | $0.128 \pm 0.049$ | [0, 0.149] | [0, 0.210] |
| 0.15 | N-point | 0.143 | $0.153 \pm 0.049$ | [0.128, 0.175] | [0.075, 0.237] |

**Table 2** Same as Table 1, but for the expected *Planck* pseudo power spectra with two-step reionization.

| Fiducial $r$ | Reionization model | Best-fit | $\bar{r} \pm \sigma$ | 68% CL | 95% CL |
|---|---|---|---|---|---|
| 0.1 | Instantaneous | 0.048 | $0.070 \pm 0.039$ | [0, 0.086] | [0, 0.141] |
| 0.1 | N-point | 0.047-0.095 | $0.089 \pm 0.042$ | [0, 0.107] | [0, 0.164] |
| 0.15 | Instantaneous | 0.095 | $0.117 \pm 0.049$ | [0, 0.139] | [0, 0.200] |
| 0.15 | N-point | 0.143 | $0.140 \pm 0.048$ | [0, 0.162] | [0, 0.221] |

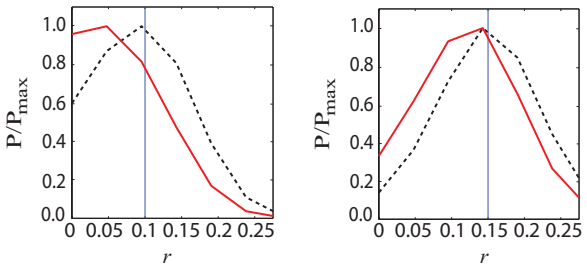


**Fig. 5** 1D marginalized probability $P$ of $r$ (relative to the peak value $P_{\rm max}$) in MCMC fitting of the expected *Planck* pseudo power spectra with double reionization as the fiducial model. The left and right panels show fiducial $r = 0.1$ and $r = 0.15$ (*indicated by vertical lines*), respectively. The solid and dashed lines stand for results of the instantaneous and N-point parameterizations respectively.

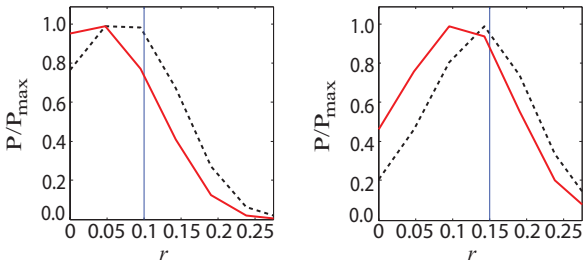


**Fig. 6** Same as Fig. 5, but with two-step reionization as the fiducial model.

Figures 7 and 8 show the corresponding 2D contours for $r$ vs. $n_{\rm s}$. In these 2D cases, the true values of $r$ and $n_{\rm s}$ are not ruled out at the 68% CL and 95% CL for both the N-point method and instantaneous reionization assumption applied in the analysis.

However, the N-point method has its own limitation when $r$ is small. Figure 9 shows the 1D marginalized probability distribution of $r$ with the fiducial $r = 0.05$. It can be seen that the marginal-

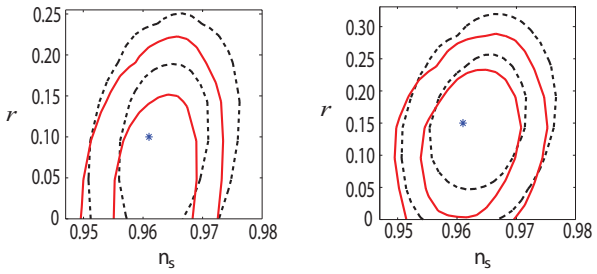


**Fig. 7** 2D marginalized probability contours of $r$ vs. $n_{\rm s}$ (68% CL and 95% CL) in the MCMC fitting of the expected *Planck* pseudo power spectra with double reionization as the fiducial model. The left and right panels show the results with the fiducial $r = 0.1$ and $r = 0.15$, respectively. The solid and dashed lines stand for results of the instantaneous and N-point parameterizations respectively. The asterisks indicate the fiducial values.

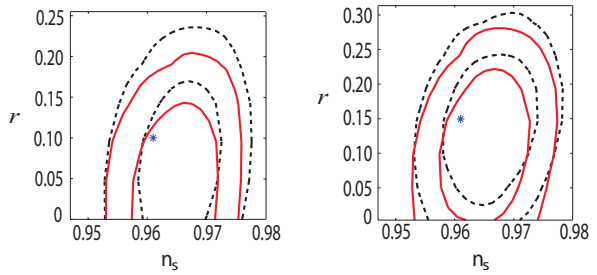


**Fig. 8** Same as Fig. 7, but with the two-step reionization as the fiducial model.

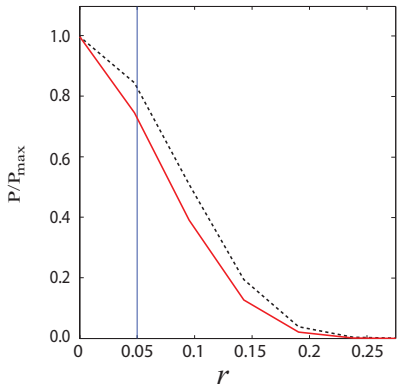


**Fig. 9** 1D marginalized probability $P$ of $r$ (relative to the peak value $P_{\rm max}$) in the MCMC fitting of the expected *Planck* pseudo power spectra with two-step reionization as the fiducial model, with $r = 0.05$ (*indicated by a vertical line*). The solid and dashed lines stand for results of the instantaneous and N-point parameterizations respectively.

ized probability of the fitted $r$ still prefers $r = 0$, which indicates that if the N-point method is applied, the *Planck* data cannot by themselves be used to detect $r$ if its value is close to 0.

Figures 10 and 11 show the fitting result of cosmological parameters applying the N-point method for the fiducial $r = 0.1$ and 0.15 respectively (we do not repeat the similar results from $r = 0.05$). It shows that the N-point method with H.L. likelihood also gives reasonable results for

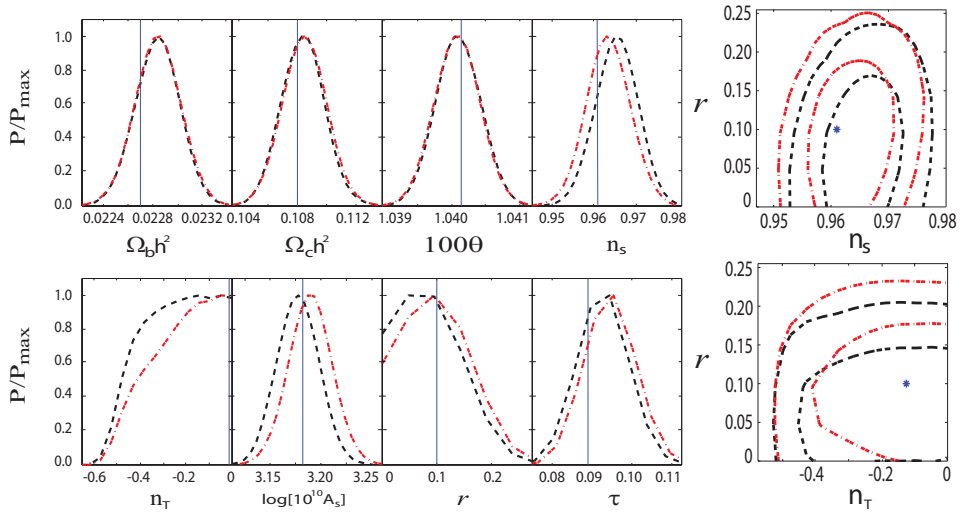


**Fig. 10** *Left*: 1D marginalized probability $P$ of cosmological parameters (relative to the peak value $P_{\rm max}$) using the N-point method in the MCMC fitting of two sets of the expected *Planck* pseudo power spectra with fiducial $r$ = 0.1 but with two-step reionization (*dashed lines*) and double reionization (*dash-dotted lines*). The vertical lines indicate the fiducial values. Right: The corresponding 2D marginalized probabilities of $r$ vs. $n_{\rm s}$ and $r$ vs. $n_{\rm T}$. The asterisks indicate the fiducial values.

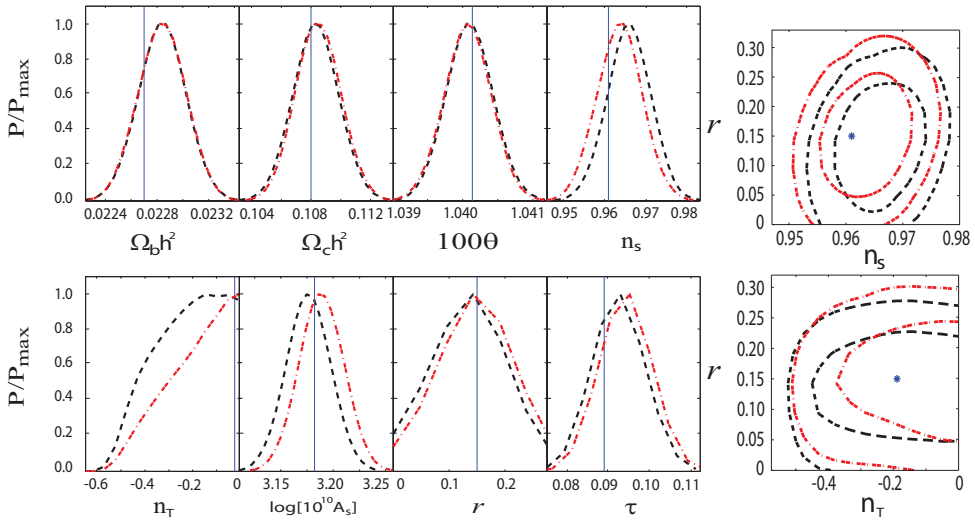


**Fig. 11** Same as Fig. 10, but for $r = 0.15$.

the fitting of other cosmological parameters ($\Omega_b h^2, \Omega_c h^2, \theta, n_{\rm s}$ and $\log(10^{10} A_{\rm s})$). By contrast, $\tau$ is still biased with its true value being ruled out at the 68% CL. This is because $\tau$ is sensitive to the MCMC fitting result for the reionization points ($\{X_e(z_i)\}_{i=1}^{N}$) for $N = 7$) as it is obtained by computing an integration over $X_e(z)$ (Eq. (1)), but our results show poor convergence for them, which means the constraints on the reionization history itself are poor based on *Planck*'s power spectra alone. However, the constraint on $r$ does give satisfactory results in the general reionization sce-

nario by marginalization since $C_l^{\rm BB}$ is not as sensitive as $\tau$ to the $N$ reionization points, as shown in Figure 2.

The 2D contours for $r$ vs. $n_{\rm s}$ and $r$ vs. $n_{\rm T}$ are also shown in the same graphs as they can be used to discriminate among inflation models and check for the consistency relation. The true values of $r$, $n_{\rm s}$ and $n_{\rm T}$ are not ruled out at 68% CL and 95% CL for both two-step reionization and double reionization. These contours also show that even with *Planck*-quality data, a large degeneracy still exists among $r$, $n_{\rm s}$ and $n_{\rm T}$.

## 5 CONCLUSIONS

It has been pointed out that $r$ can be biased by an incorrect assumption about reionization history. In this paper, we consider the general reionization scenario by studying double reionization and two-step reionization models. We apply the H.L. likelihood approximation to give an idealized constraint of $r$ for the expected *Planck* cut-sky power spectra. We found that the estimation of $r$ is possibly biased by an overly simplistic instantaneous reionization model. The N-point linear interpolation model of reionization can correct this bias if $r \gtrsim 0.1$. On the other hand, if $r \lesssim 0.1$, not even the N-point method can produce an accurate inference of $r$ from the *Planck* data, given current uncertainties in $X_e(z)$.

To calculate the expected *Planck* power spectrum, we simply add the fiducial power spectrum with the appropriate beam factor and noise spectrum, following the multiplication of mask matrices, as shown in Equation (11). We did not extract the power spectrum from a CMB sky-map generated randomly according to a Gaussian distribution, as our focus is on the analysis method applied to account for the reionization history. Unlike the sky-map approach, which should have $\sim 1\sigma$ scatters from the input in the inference on cosmological parameters even if the correct cosmic model is applied, we found that the outcome of $r$ is sharply peaked at its fiducial value up to $r = 0.05$ when the assumption on reionization is correct. Thus, our approach highlights that deviations shown by the inference on $r$, if present, are due to the incorrect assumption on cosmic reionization rather than randomness in the sky-map simulation.

Our conclusion is based on the results using $N = 7$ in the N-point method. In principle, better results may be obtained if $N$ is further increased so as to improve the modeling of the reionization history. However, it will also largely increase the convergence time for the chains in MCMC since the total numbers of varying parameters are $7 + N$. We choose $N = 7$ in order to have a reasonable balance between computation time and good representation of the reionization history.

In our method, we focus on the cut-sky estimators $P(b_l^2 C_l + N_l)$ instead of trying to recover the full-sky CMB power spectra from the cut-sky spectra by imposing the inverse of the WMAP mask matrices $\{M_{ll'}^{XY}\}$. This is because the matrices $\{M_{ll'}^{XY}\}$ are almost singular and imposing their inverse on the cut-sky power spectra amplifies the noise in them and thus worsens the forecast. One of the advantages of applying the H.L. likelihood is that we can change the CMB full-sky estimators in it to be the cut-sky ones.

We omit the band-power, multiple frequency estimators and the anisotropic noises here. Moreover, we extend the application of the H.L. likelihood to $l_{\rm min} = 2$ for making the forecast, while the likelihood computed from the Internal Linear Combination maps is usually applied in the range $l \leq 30$ in practice (Dunkley et al. 2009; Larson et al. 2011). These factors may further limit the accuracy of the constraints on $r$. We also omit the contamination of the B-mode power spectrum by the gravitational lensing effect as it is expected to be removed (Seljak & Hirata 2004). In the future, we would like to explore this problem using a more realistic method, for instance, using the full likelihood in the low-$l$ range and model the *Planck*-quality data from a simulated CMB sky-map.

**Acknowledgements** This work is partially supported by a grant from the Research Grant Council of the Hong Kong Special Administrative Region, China (Project No. 400910). J. TANG is grateful for the support of a postdoctoral fellowship by The Chinese University of Hong Kong. We also

thank the ITSC of The Chinese University of Hong Kong for providing clusters that were used for computations.

## Appendix A: HAMIMECHE-LEWIS LIKELIHOOD

The H.L. likelihood approximation gives the maximum likelihood function (Hamimeche & Lewis 2008) as

$$-2\ln\mathcal{L} = \mathbf{X}_g^{\mathrm{T}}\mathbf{M}_f^{-1}\mathbf{X}_g = \sum_{ll'}[\mathbf{X}_g]_l^{\mathrm{T}}[\mathbf{M}_f^{-1}]_{ll'}[\mathbf{X}_g]_{l'}\,, \tag{A.1}$$

where $\mathbf{M}_f$ is the covariance block matrix for $\mathbf{X}_l = \mathrm{vecp}(\mathbf{C}_l)$ (a vector of all distinct elements of matrix $\mathbf{C}_l$) and is evaluated for some specific fiducial model $\{C_l\} = \{C_{fl}\}$. It contains $(l_{\mathrm{max}} - l_{\mathrm{min}} + 1) \times (l_{\mathrm{max}} - l_{\mathrm{min}} + 1)$ blocks labeled by $l$ and $l^{'}$, and $\mathbf{X}_g$ is generally a $(l_{\mathrm{max}} - l_{\mathrm{min}} + 1) \times 6$ row block vector:

$$[\mathbf{M}_f]_{ll'} = \langle(\hat{\mathbf{X}}_l - \mathbf{X}_l)(\hat{\mathbf{X}}_{l'} - \mathbf{X}_{l'})^{\mathrm{T}}\rangle_f\,, \tag{A.2}$$

$$[\mathbf{X}_g]_l = \mathrm{vecp}\left(\mathbf{C}_{fl}^{1/2} g[\mathbf{C}_l^{-1/2}\hat{\mathbf{C}}_l\mathbf{C}_l^{-1/2}]\mathbf{C}_{fl}^{1/2}\right)\,, \tag{A.3}$$

$$\mathbf{C}_l = \begin{pmatrix} C_l^{\mathrm{TT}} & C_l^{\mathrm{TE}} & C_l^{\mathrm{TB}} \\ C_l^{\mathrm{TE}} & C_l^{\mathrm{EE}} & C_l^{\mathrm{EB}} \\ C_l^{\mathrm{TB}} & C_l^{\mathrm{EB}} & C_l^{\mathrm{BB}} \end{pmatrix}\,, \tag{A.4}$$

$$\mathbf{C}_{fl} = \begin{pmatrix} C_{fl}^{\mathrm{TT}} & C_{fl}^{\mathrm{TE}} & C_{fl}^{\mathrm{TB}} \\ C_{fl}^{\mathrm{TE}} & C_{fl}^{\mathrm{EE}} & C_{fl}^{\mathrm{EB}} \\ C_{fl}^{\mathrm{TB}} & C_{fl}^{\mathrm{EB}} & C_{fl}^{\mathrm{BB}} \end{pmatrix} \tag{A.5}$$

for $l, l^{'} = l_{\mathrm{min}}, \cdots, l_{\mathrm{max}}$, where

$$g(x) \equiv \mathrm{sign}(x-1)\sqrt{2(x - \ln x - 1)}\,, \tag{A.6}$$

$$[g(\mathbf{A})]_{ij} = \begin{cases} g(\mathbf{A}_{ii})\delta_{ij} & \mathbf{A} \text{ is diagonal} \\ [\mathbf{U}g(\mathbf{D})\mathbf{U}^{\mathrm{T}}]_{ij} & \mathbf{A} \text{ is symmetric positive-definite} \end{cases} \tag{A.7}$$

(then $\mathbf{A} = \mathbf{U}\mathbf{D}\mathbf{U}^{\mathrm{T}}$ for some diagonal matrix $\mathbf{D}$). The assumption $C_l^{\mathrm{TB}} = C_l^{\mathrm{EB}} = 0$ is applied in our study. Equation (A.1) gives the exact results for the full sky $C_l$. Moreover, it has been tested to be reliable in the range $30 < l < 2000$ when used on the masked-sky spectra $P(C_l)$. To deal with the cut-sky effect, all of the full-sky power spectra $C_l$ described above are changed such that

$$C_l \to P(b_l^2 C_l + N_l). \tag{A.8}$$

For the computation of the covariance matrix $\mathbf{M}_f$, the fiducial model we applied is based on the same cosmological parameters as the input, since they are well constrained by present cosmological surveys, but we fixed $r = 0.15$ and used the instantaneous reionization model with $\tau = 0.089$ and $z_{re} = 10.5$. Using HEALPix[5] (Górski et al. 2005), we can compute $\mathbf{M}_f$ by generating random samples from the same $C_l$ power spectra. As there are $p = 6 \times (l_{\mathrm{max}} - l_{\mathrm{min}} + 1)$ estimators in $\{\mathbf{X}_l\}_l$, we generate $1.5 \times 10^5$ random samples in order to have a good convergence, following the $N_{\mathrm{sample}} \sim p \ln p$ rule (Vershynin 2012).

[5] HEALPix is available at *http://healpix.sourceforge.net/*

## References

Albrecht, A., & Steinhardt, P. J. 1982, Physical Review Letters, 48, 1220
Becker, R. H., Fan, X., White, R. L., et al. 2001, AJ, 122, 2850
Belikov, A. V., & Hooper, D. 2009, Phys. Rev. D, 80, 035007
Bennett, C. L., Larson, D., Weiland, J. L., et al. 2013, ApJS, 208, 20
Bunker, A. J., Stanway, E. R., Ellis, R. S., & McMahon, R. G. 2004, MNRAS, 355, 374
Burigana, C., Destri, C., de Vega, H. J., et al. 2010, ApJ, 724, 588
Dodelson, S., Kinney, W. H., & Kolb, E. W. 1997, Phys. Rev. D, 56, 3207
Dunkley, J., Komatsu, E., Nolta, M. R., et al. 2009, ApJS, 180, 306
Fan, X., Narayanan, V. K., Strauss, M. A., et al. 2002, AJ, 123, 1247
Górski, K. M., Hivon, E., Banday, A. J., et al. 2005, ApJ, 622, 759
Guth, A. H. 1981, Phys. Rev. D, 23, 347
Hamimeche, S., & Lewis, A. 2008, Phys. Rev. D, 77, 103013
Hinshaw, G., Larson, D., Komatsu, E., et al. 2013, ApJS, 208, 19
Hu, W., & White, M. 1996, Physical Review Letters, 77, 1687
Hu, W., Spergel, D. N., & White, M. 1997, Phys. Rev. D, 55, 3288
Jarosik, N., Bennett, C. L., Dunkley, J., et al. 2011, ApJS, 192, 14
Kamionkowski, M., Kosowsky, A., & Stebbins, A. 1997, Physical Review Letters, 78, 2058
Kinney, W. H. 1998, Phys. Rev. D, 58, 123506
Kogut, A., Spergel, D. N., Barnes, C., et al. 2003, ApJS, 148, 161
Kosowsky, A., Milosavljevic, M., & Jimenez, R. 2002, Phys. Rev. D, 66, 063007
Larson, D., Dunkley, J., Hinshaw, G., et al. 2011, ApJS, 192, 16
Lewis, A., Challinor, A., & Lasenby, A. 2000, ApJ, 538, 473
Lewis, A., & Bridle, S. 2002, Phys. Rev. D, 66, 103511
Lewis, A., Weller, J., & Battye, R. 2006, MNRAS, 373, 561
Linde, A. D. 1982, Physics Letters B, 108, 389
Mapelli, M., Ferrara, A., & Pierpaoli, E. 2006, MNRAS, 369, 1719
Moradinezhad Dizgah, A., Gnedin, N. Y., & Kinney, W. H. 2013, J. Cosmol. Astropart. Phys., 5, 017
Mortonson, M. J., & Hu, W. 2008a, Phys. Rev. D, 77, 043506
Mortonson, M. J., & Hu, W. 2008b, ApJ, 672, 737
Pandolfi, S., Giusarma, E., Kolb, E. W., et al. 2010, Phys. Rev. D, 82, 123527
Peiris, H. V., Komatsu, E., Verde, L., et al. 2003, ApJS, 148, 213
Planck Collaboration 2006, arXiv:astro-ph/0604069
Planck Collaboration, Ade, P. A. R., Aghanim, N., et al. 2013a, arXiv:1303.5062
Planck Collaboration, Ade, P. A. R., Aghanim, N., et al. 2013b, arXiv:1303.5082
Sasaki, S., & Umemura, M. 1996, ApJ, 462, 104
Seljak, U., & Zaldarriaga, M. 1997, Physical Review Letters, 78, 2054
Seljak, U., & Hirata, C. M. 2004, Phys. Rev. D, 69, 043005
Spergel, D. N., & Zaldarriaga, M. 1997, Physical Review Letters, 79, 2180
Spergel, D. N., Bean, R., Doré, O., et al. 2007, ApJS, 170, 377
Springel, V., & Hernquist, L. 2003, MNRAS, 339, 312
Story, K. T., Reichardt, C. L., Hou, Z., et al. 2013, ApJ, 779, 86
Vershynin, R. 2012, Journal of Theoretical Probability, 25, 655
Zahn, O., Reichardt, C. L., Shaw, L., et al. 2012, ApJ, 756, 65